RAPID COMMUNICATIONS

PHYSICAL REVIEW C VOLUME 52, NUMBER 2 AUGUST 1995

# Study of the $^{18}F(p,\alpha)^{15}O$ reaction at astrophysical energies using a $^{18}F$ beam

K. E. Rehm,[1] M. Paul,[2] A. D. Roberts,[3] D. J. Blumenthal,[1] J. Gehring,[1] D. Henderson,[1] C. L. Jiang,[1] J. Nickles,[3] J. Nolen,[1] R. C. Pardo,[1] J. P. Schiffer,[1] and R. E. Segel[4]

[1]*Argonne National Laboratory, Argonne, Illinois 60439*

[2]*Hebrew University, Jerusalem, Israel 91 904*

[3]*University of Wisconsin, Madison, Wisconsin 53706*

[4]*Northwestern University, Evanston, Illinois 60208*

(Received 1 February 1995; revised manuscript received 10 April 1995)

For the first time the $^{18}F(p,\alpha)^{15}O$ reaction has been studied with a $^{18}F$ beam at energies which are of interest to explosive nucleosynthesis. Utilizing the gas-filled magnet technique a clean identification of the reaction products was achieved. A resonance with spin $3/2^+$ at an equivalent c.m. energy of 660 keV dominates the yield.

PACS number(s): 25.70.Hi, 25.40.Hs, 25.60.+v, 95.30.Cq

A number of interesting issues in nuclear astrophysics as well as in nuclear structure can best be addressed by the use of radioactive ion beams. The main difficulties in these experiments, compared to studies performed with beams of stable particles, are the much lower intensities of the available beams which often have stable isobars as impurities. These difficulties require the use of highly efficient detection systems capable of separating the reactions induced by the particles of interest from the ones induced by the beam contaminant(s) even at low energies.

Examples of recent studies using radioactive beams for experiments of interest to astrophysics are cross-section measurements for the $^{13}N(p,\gamma)^{14}O$ and $^{19}Ne(p,\gamma)^{20}Na$ reactions with $^{13}N$ and $^{19}Ne$ beams, respectively [1,2]. Similar experiments with $^{14,15}O$ and $^{17,18}F$ beams which are important for the hot CNO cycle are considerably more difficult because of the highly reactive chemical properties of these elements. In this contribution we report on the first measurement of the $^{18}F(p,\alpha)^{15}O$ reaction using a radioactive $^{18}F$ beam.

Explosive nucleosynthesis occurs under extreme temperature and density conditions at various sites, including novas, supernovas, and x-ray bursts [3]. Network calculations [3] of the $rp$ process, i.e., a sequence of $(p,\gamma)$ reactions followed by $\beta^+$ decays, show that one of the crucial isotopes in this process is $^{19}Ne$, which can be produced in two ways: (i) a direct one-step method via the $^{15}O(\alpha,\gamma)^{19}Ne$ reaction or (ii) with a more complicated path involving the breakout from the hot CNO cycle via the sequence $^{14}O(\alpha,p)^{17}F(p,\gamma)^{18}Ne(\beta^+)^{18}F(p,\gamma)^{19}Ne$. The latter sequence, however, can be interrupted by the $^{18}Fe(p,\alpha)^{15}O$ reaction leading back to nuclei of the CNO cycle. Measurements of the $^{18}F(p,\alpha)$ and $^{18}F(p,\gamma)$ yields at low energies will therefore give valuable information about the contribution of the CNO-breakout route to the production of $^{19}Ne$. Some of the information relevant to the above sequence can be obtained in the form of energies and widths of resonances using stable beams and targets [3]. Radioactive ion beams, however, provide the only method for directly measuring the relevant cross sections and, in particular, the nonresonant part of the reaction cross sections.

The measurement of the $^{18}F(p,\alpha)^{15}O$ reaction was carried out with a $^{18}F$ beam of a few ppA from the Argonne tandem accelerator (one of the injectors to ATLAS), using for detection of the $^{15}O$ reaction products the gas-filled magnet technique which is described below. Because of the relatively long half-life of $^{18}F$ ($T_{1/2}=110$ min) it was possible to use a two-step procedure for the beam production. $^{18}F$, which is a well-studied PET isotope, is generated at the medical cyclotron of the University of Wisconsin. Aqueous [$^{18}F$] fluoride ions are produced via the $^{18}O(p,n)^{18}F$ reaction using a 30 $\mu$A, 11.4 MeV proton beam bombarding a 95% enriched [$^{18}O$] water target and are electroplated onto the end of a 3-mm-diam Al anode. Details of the production method will be published separately [4]. After electroplating, the anodized Al is pressured into a copper cathode insert for a National Electrostatics Corporation SNICS ion source, transported to Argonne National Laboratory and installed in the ion source of the Tandem accelerator at ATLAS. With an activity at the end of the electroplating process of 530 mCi the starting activity after 2 h, which is the time needed to transport and install the material in the SNICS source, was 250 mCi, corresponding to a total number of $^{18}F$ atoms of $8.8\times10^{13}$.

The $^{18}F^-$ ions extracted from the ion source were accelerated to energies between 11.7–15.1 MeV in the tandem accelerator using the $4^+$ charge state. This energy range was chosen since recent measurements of the $^{19}F(^3He,t)^{19}Ne$ reaction [5] found a broad state in $^{19}Ne$ at an excitation energy of about 7.07 MeV. The yield of $^{15}O$ from the $^1H(^{18}F,\alpha)^{15}O$ reaction is focused in the forward direction by the inverse reaction kinematics. The solid angle in the laboratory is greater by a factor of 30 than in the center of mass and, thus, detecting $^{15}O$ with a given detector is an order of magnitude more favorable than detecting the $\alpha$'s from this reaction. In order to make use of this increase in detection efficiency for inverse reactions, however, a particle identification system is required which can separate the heavy reaction products $^{15}O$ and $^{18}F$ from other heavy particles such as $^{12}C$, $^{15}N$, and $^{18}O$.

The main difficulty in the experiment is associated with the presence of an $^{18}O$ admixture in the $^{18}F$ ion beam. Although much care is taken to remove most of the $^{18}O$ enriched water used in the production process, the removal is not complete. In addition, $^{18}O$ gas is present in the ion

 

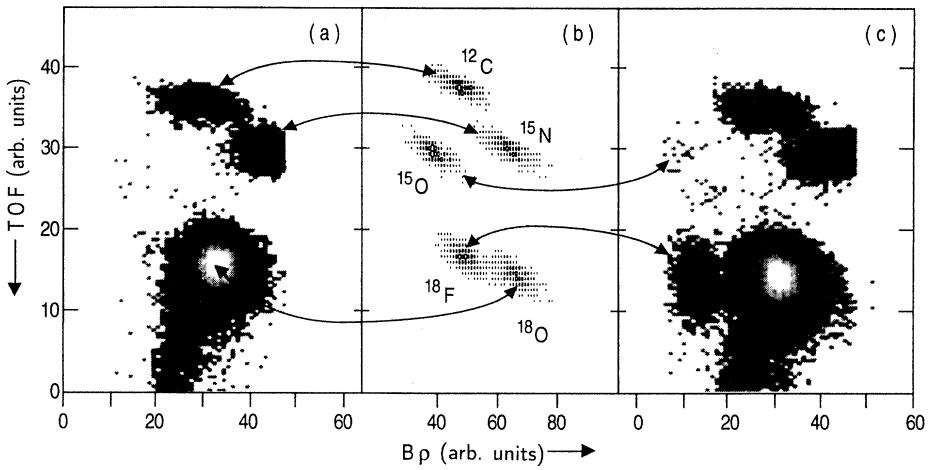


FIG. 1. (a) Two-dimensional plot of time-of-flight (TOF) versus magnetic rigidity ($B\rho$) measured with the gas-filled magnet for 13.4 MeV $^{18}O$ ions bombarding a polypropylene target. (b) RAYTRACE calculation for various ions in a gas-filled magnet. See text for details. (c) Same as (a) but with a mixed $^{18}F$-$^{18}O$ sample in the ion source.

source from the natural abundance in air (0.2%). Because of the very small mass difference between $^{18}F$ and $^{18}O$ ($\Delta m/m < 10^{-4}$) magnetic separation of the $^{18}F^{4+}$ from the $^{18}O^{4+}$ ions is not feasible. While the $^{18}O$ beam contamination has the beneficial effect of providing a guide beam for stabilizing the terminal voltage of the tandem accelerator and monitoring beam transmission, it also increases the number of reaction products which need to be separated by the detection system. At bombarding energies of about 700 keV/$u$, the $Q$ values of $^{18}F$, $^{18}O$ induced reactions restrict the spectrum of heavy ion reaction products to $^{18}O$, $^{18}F$ (from elastic scattering), $^{15}N$, $^{15}O$ [from the $^{18}O$ and $^{18}F$ induced $(p,\alpha)$ reactions] and all possible recoil ions which are present in the target. In order to keep the number of recoil products to a minimum, a polypropylene target with a thickness of 118 $\mu$g/cm$^2$ was chosen, adding $^{12}C$ and $^{16}O$ (from a small water contamination) to the list.

While good mass separation of these slow particles can be achieved with a time-of-flight measurement, the large intensity differences expected between $^{18}O$ and $^{18}F$ or $^{15}N$ and $^{15}O$, require a $Z$-identification method that can reliably separate these particles even at energies well below the Bragg maximum. Since normal $\Delta E - E$ techniques do not have sufficient resolving power at low energies, we have used the method of a gas-filled magnet for $Z$ identification of low-energy heavy ions [6–8].

In a gas-filled magnetic field ions experience charge changing collisions with the gas molecules which result in an average charge state $\bar{q}$ which, in the parametrization of Dmitriev *et al.* [9], is given in

$$\bar{q} = Z \cdot \ln\left(2.43 \frac{v}{v_0} \frac{1}{Z^{0.4}}\right) \Big/ \ln(7 \cdot Z^{0.3}),$$

where $v$ is the velocity of the ions, $Z$ their nuclear charge, and $v_0$ the Bohr velocity, respectively. At the optimum gas pressure [7] the width of the charge state distribution $\Delta q/q$ is typically 2%. This width is small enough to allow a measurement of the full yield of the change state distribution with a relatively small focal plane detector. Introducing the equation for the average charge state into the expression for the magnetic rigidity one obtains a $Z$ dependence of $B\rho = mv/\bar{q}$ which is valid to very low velocities and allows a separation of isobars even for cases with very large differences in intensities [10].

For the experiment the Enge split-pole spectrograph was filled with $N_2$ gas at a pressure of 0.5 Torr. A $1 \times 1$ cm$^2$ parallel-grid-avalanche-counter (PGAC) at the entrance of the magnet provided a start signal for the time-of-flight measurement and also served as a pressure foil separating the gas in the magnet from the vacuum in the scattering chamber. The particles were detected in the focal plane with a $50 \times 10$ cm$^2$ PGAC [11], which was sufficiently far away from target and beam stop, that the background generated by the $\beta^+$ decay of $^{18}F$ was greatly reduced and very clean identification spectra were obtained.

A spectrum of time-of-flight (TOF) vs magnetic rigidity ($B\rho$) measured at a scattering angle of $\theta_{lab} = 13°$ for a 13.4 MeV $^{18}O$ beam bombarding a 118 $\mu$g/cm$^2$ polypropylene target is shown in Fig. 1(a). The three groups of particles seen are attributed to elastically scattered $^{18}O$ ions, $^{15}N$ ions from the $^{18}O$ $(p,\alpha)$ reaction and $^{12}C$ recoil ions. This identification was verified in a series of test measurements by generating recoil particles with the appropriate targets. In the same way the locations of $^{19}F$, $^{16}O$, $^{14}N$, and $^{13}C$ ions in the TOF vs $B\rho$ plane were determined. The assignment of the various particle groups was verified by RAYTRACE calculations which in a Monte Carlo treatment take charge-changing collisions, energy-loss, and straggling effects into account [7]. A spectrum calculated for the split-pole spectrograph for $^{12}C$, $^{15}N$, $^{15}O$, $^{18}O$, and $^{18}F$ ions is shown in Fig. 1(b). This calculation reproduces qualitatively the relative location of $^{12}C$, $^{18}O$, and $^{15}N$ ions and, furthermore, predicts the location of the $^{18}F$ and $^{15}O$ groups which cannot be generated as recoil ions from elastic scattering. Figure 1(c) shows the spectrum obtained by scattering $^{18}O$ and $^{18}F$ ions from a polypropylene target when the 250 mCi $^{18}F$ sample was installed in the ion source. A comparison of Figs. 1(a) and 1(c) clearly shows excess counts in the area where $^{18}F$ and $^{15}O$ ions are expected. The count rate of the $^{15}N$, $^{16}O$, and $^{12}C$ events normalized to $^{18}O$ remained constant in time while the $^{18}F$ and $^{15}O$ rates decreased with half-lives of $90 \pm 20$ min and $150 \pm 140$ min, respectively.

The background counts observed in the $^{15}O$ region with a pure $^{18}O$ beam were investigated under various experimental

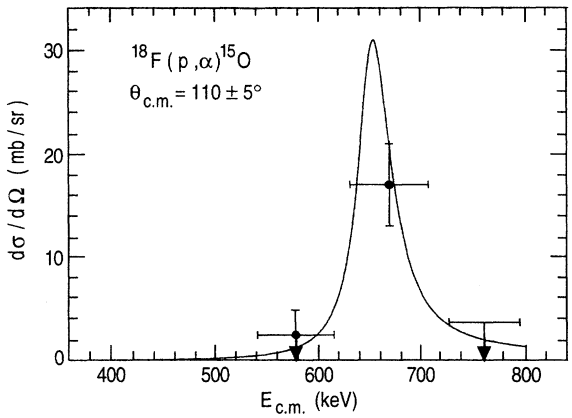


FIG. 2. Cross section measured at three energies for the $^{18}F(p,\alpha)^{15}O$ reaction at $\theta_{c.m.}=110\pm5°$. The solid line corresponds to a resonance at an excitation energy of 7.066 MeV in $^{19}Ne$ with parameters given in Table I. The point at 660 keV represents the average of three measurements, one taken just before the 580- and 760-keV points and one after. The horizontal bars reflect the energy interval covered by the target thickness.

conditions, including various targets and higher intensity $^{18}O$ currents. The background was found to be caused by the low-energy tail originating at the location of the $^{12}C$ recoils. These tails, which are also seen extending from the $^{15}N$ and $^{18}O$ groups, have a typical intensity ratio of $2\times10^{-3}$ with respect to the main peak. They are caused by scattering of the particles in the start detector and the $N_2$ gas in the magnet and are discussed in more detail in Ref. [12].

The average $^{18}F$ beam intensity can be calculated from a comparison of the $^{18}F$ and $^{18}O$ events which are caused by elastic scattering on the $^{12}C$ component of the polypropylene target. For the time-averaged $^{18}F$ intensity hitting the polypropylene target one obtains $2.3\times10^5$ ions/sec while the $^{18}O$ beam was about 240 times more intense. With the transmission efficiency from the ion source to target of 3%, measured with an $^{18}O$ beam of the same energy, and taking the difference in stripping efficiency for oxygen and fluorine ions into account an initial $^{18}F$ current at the ion source of 2 ppA is calculated.

The bombarding energy range in the experiment was chosen to cover a state at $E_x=7.066$ MeV excitation energy in $^{19}Ne$, which has been seen in the ($^3$He,$t$) [5] reaction with a total width of about 40 keV. From a comparison with the mirror nucleus $^{19}F$, the 7.066 state in $^{19}Ne$ could be the analogue of the 7.114 MeV $7/2^+$ state in $^{19}F$ which has an $\alpha$ width of $\sim$32 keV [13]. Other states in $^{19}F$ in this energy range with similar widths are the $1/2^-$ state at 6.989 MeV ($\Gamma\simeq51$ keV) or the $3/2^+$ state at 6.891 MeV ($\Gamma\simeq28$ keV) [13].

The results of the energy dependence of the $^{18}F(p,\alpha)^{15}O$ reaction are shown in Fig. 2 where the c.m. cross section is plotted as function of the c.m. energy. A strong energy dependence is observed. The horizontal bars represent the target thickness of the $CH_2$ target which was measured before and after the experiment with an $^{241}Am$ source. The solid line represents a resonance at $E_x=7.066$ MeV with a resonance strength which will be discussed below. At the higher bombarding energy no $^{15}O$ events were detected and the cross-section value represents an upper limit only. This also sets an upper limit to the contribution from nonresonant processes in this energy region of $\sigma_{nr}<3.6$ mb/sr.

TABLE I. Proton and $\alpha$ widths for the 7.066 keV state in $^{19}Ne$ extracted from the data under the assumption that the yield is entirely from a single resonance with a width of 40 keV (Ref. [5]). Single particle estimates assuming different spin assignments are also included.

| Spin | $\Gamma_p^{exp}$ (keV) | $\Gamma_p$ Wigner limit (keV) | $\Gamma_\alpha^{exp}$ (keV) | $\Gamma_p$ (from $^{19}F$) (keV) |
|---|---|---|---|---|
| $7/2^+$ | $3\pm0.8$ | 0.32 | 37 | 37 |
| $1/2^-$ | $16\pm4$ | 7.7 | 24 | 59 |
| $3/2^+$ | $6.7^{+2.2}_{-1.9}$ | 45.9 | 33 | 12 |

The widths $\Gamma_p$ and $\Gamma_\alpha$ calculated from the resonance strength $\omega\gamma=3.7\pm0.9$ keV for various spin assignments are summarized in Table I using the value of 40 keV for the total width as measured in [5]. Since the $\alpha$-particle widths of $^{19}Ne$ states are related to those in $^{19}F$ by isospin symmetry the values of $\Gamma_\alpha$ calculated from the $^{19}F$ values, corrected for the different penetrability, are also shown. For comparison, the single-particle limits calculated for the corresponding $l$ transfers are also included. The first two spin choices, while yielding $\alpha$ widths consistent with those of resonance with the corresponding spins in $^{19}F$, would require proton widths that exceed the single-particle limit for proton decay. This rules out a $7/2^+$ assignment and makes the $3/2^-$ and $1/2^-$ assignments unlikely. Only for spins $3/2^+$ and $1/2^+$, formed with $s$-wave protons, are the extracted protons widths consistent with the Wigner limit. (Since the 40 keV total width is close to the experimental resolution of Ref. [5], a smaller total width is not out of the question; this would increase the proton width extracted; $\Gamma_\alpha=12$ keV would yield $\Gamma_p=10$ keV and $\Gamma=22$ keV.) It is interesting to note than an early measurement of the $^{15}N(\alpha,\alpha)$ reaction [14] identified a $7/2^+$, $3/2^+$ doublet at $E_x=7.1$ MeV in $^{19}F$, though a later analysis questioned the need for the $3/2^+$ resonance [15]. The solid line in Fig. 2 is calculated assuming a $3/2^+$ resonance at 7.066 MeV in $^{19}Ne$ and is in good agreement with the measured data.

We have succeeded in a first measurement with a radioactive $^{18}F$ beam, utilizing a two-step process with two accelerators in different locations and the gas-filled magnet technique. We have found an $s$-wave resonance in the $^{18}F(p,\alpha)$ reaction that is likely to have a dominant role for this reaction at lower energies. Further improvements in the efficiency of the ion source and the transmission of the ATLAS accelerator by a factor of 10 are possible. This would allow an extension of the $(p,\alpha)$ reaction to lower energies and a measurement of the $^{18}F(p,\gamma)$ reaction.

This work was supported in part by the U.S. Department of Energy, Nuclear Physics Division, under Contract No. W-31-109-ENG-38 and by the National Science Foundation under Grant No. PHY-9412680.

[1] P. DeCrock *et al.*, Phys. Rev. Lett. **67**, 808 (1991).
[2] R. D. Page *et al.*, Phys. Rev. Lett. **73**, 3066 (1994).
[3] A. E. Champagne and M. Wiescher, Annu. Rev. Nucl. Part. Sci. **42**, 39 (1992).
[4] A. D. Roberts *et al.*, Proceedings of the 13th International Conference on the Application of Accelerators in Research and Industry, Denton, TX, 1994 [Nucl. Instrum. Methods Res. Sect. B (to be published)].
[5] P. Parker, First Symposium on Nuclear Physics in the Universe, Oak Ridge, TN, 1992; M. Wiescher (private communication).
[6] B. L. Cohen and C. B. Fulmer, Nucl. Phys. **6**, 547 (1958).
[7] W. Henning *et al.*, Science **236**, 725 (1987); M. Paul *et al.*, Nucl. Instrum. Methods Res. Sect. A **277**, 418 (1989).
[8] F. Scarlassara *et al.*, Nucl. Instrum. Methods Res. Sect. A **309**, 485 (1991).
[9] I. S. Dmitriev *et al.*, Sov. Phys. JETP **20**, 409 (1965).
[10] W. Kutschera *et al.*, Nucl. Instrum. Methods Res. Sect. B **92**, 241 (1994).
[11] K. E. Rehm *et al.*, Nucl. Instrum. Methods Res. Sect. A **344**, 614 (1994).
[12] T. R. Ophel *et al.*, Nucl. Instrum. Methods Res. Sect. A **272**, 734 (1988).
[13] F. Ajzenberg-Selove, Nucl. Phys. **A475**, 1 (1987).
[14] H. Smotrich *et al.*, Phys. Rev. **122**, 232 (1961).
[15] T. Mo *et al.*, Nucl. Phys. **A198**, 153 (1972).

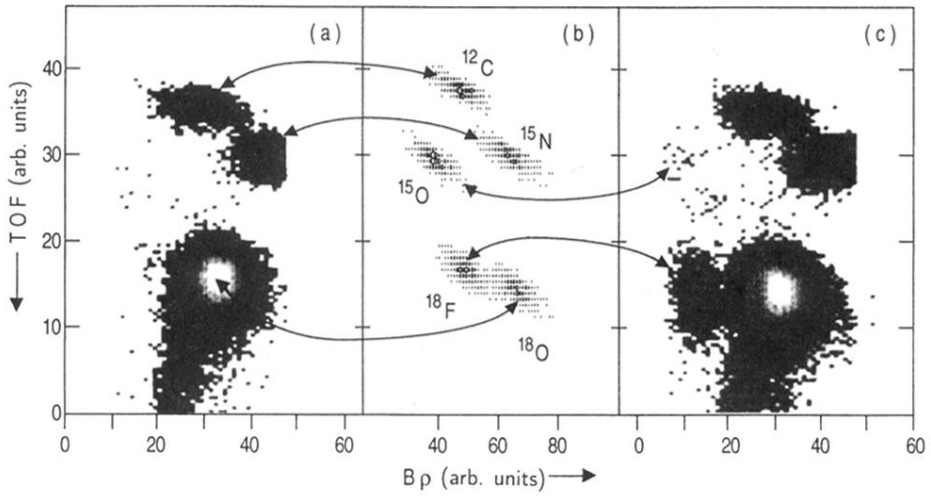


FIG. 1. (a) Two-dimensional plot of time-of-flight (TOF) versus magnetic rigidity ($B\rho$) measured with the gas-filled magnet for 13.4 MeV $^{18}$O ions bombarding a polypropylene target. (b) RAYTRACE calculation for various ions in a gas-filled magnet. See text for details. (c) Same as (a) but with a mixed $^{18}$F-$^{18}$O sample in the ion source.